Electronic Supplementary Material (ESI) for Nanoscale Advances.

[Supplementary Information (SI)]

Tight-binding investigation of structural and vibrational properties of graphene-single wall carbon nanotube junctions

Juhi Srivastava,[a,b] and Anshu Gaur[a,b*]

S.1 Structural specifications and deformation behavior

(a)				(b)			
Hybrid	No. of Atoms			Diameter [D (Å)]	$\Delta[D_x]$ (Å)	$\Delta[D_y]$ (Å)	Dip in Graphene (Å)
	SWNT	SLG	Hybrid				
Gr-CNT(8,0)	32	64	96	6.446	0.066	-0.080	0.763
Gr-CNT(5,5)	20	36	56	6.946	0.074	-0.079	0.813
Gr-CNT(9,0)	36	60	96	7.224	0.095	-0.108	0.823
Gr-CNT(10,0)	40	64	104	8.003	0.129	-0.161	0.931
Gr-CNT(6,6)	24	36	60	8.304	0.142	-0.169	0.924
Gr-CNT(7,7)	28	40	68	9.639	0.172	-0.322	1.099
Gr-CNT(13,0)	52	64	116	10.362	0.297	-0.360	1.095
Gr-CNT(8,8)	32	40	72	11.030	0.369	-0.463	1.197
Gr-CNT(9,9)	36	44	80	12.397	0.555	-0.721	1.370
Gr-CNT(16,0)	64	64	128	12.728	0.594	-0.766	1.311
Gr-CNT(10,10)	40	48	88	13.765	0.809	-1.043	1.557
Gr-CNT(11,11)	44	48	92	15.134	1.100	-1.462	1.645

Table 1 (a) The numbers of atoms in individual SWNT and SLG and in their hybrid structures for various hetero-structures studies in this work; **(b)** Structural deformations in components (SWNT and SLG) after geometrical relaxation of the hybrid structures, shown as the variation in horizontal (ΔD_x) and vertical (ΔD_y) tube diameters and the change in y-level of graphene at the point of closest proximity between SWNT and SLG (dip). The data is sorted according to increasing diameter.

S.2 Calculation Method

Tight binding DFT methods are most suitable when dealing with large number of atoms in a system. Unlike DFT which uses a plane-wave basis set and pseudopotentials based on different approximations to replace the true wave-function of the many electron system with a smooth wave-function with no radial nodes in the core, DFTB method is based on the parameterization of pairwise atomic interactions (incorporated in Slater-Koster (S-K) files)[1]. These files include tabulated Hamiltonian, overlap matrix elements, and the repulsive potentials which are added to compute the total energies by fitting to reproduce the DFT total energy. Various S-K parameters have previously been tested for organic[1] and inorganic[2] based compounds for structural and electronic properties. While few authors have investigated the accuracy of this method for the calculation of vibrational frequencies[1,3–5], T. A. Niehaus *et al.*[6] has benchmarked this method and various Slater-Koster parameter sets for the calculations of phonon dispersion and also compared the results obtained with the available DFT results.

[a] *Department of Materials Science and Engineering, Indian Institute of Technology Kanpur, Kanpur 208016, Uttar Pradesh, India.*
[b] *Samtel Centre for Display Technologies, Indian Institute of Technology Kanpur, Kanpur 208016, Uttar Pradesh, India.*
∗ The corresponding author; *E-mail: agaur@iitk.ac.in*

S.3 Phonon frequencies in hybrid nanostructures

Hybrids	Modes	Phonon frquencies (cm^{-1})				Total Frequency shift (cm^{-1})		
GR-CNT(5,5)		Pristine (P)	Unrelaxed hybrids(U)	Relaxed hybrids(R)	Deformed components(D)	U-P	R-P	D-P
	RBM	341.43	344.46	344.05	341.48	3.03	2.61	0.05
	LO-CNT	1564.97	1564.9	1564.88	1564.87	-0.07	-0.1	-0.1
	TO-CNT	1588.27	1588.15	1587.31	1587.49	-0.13	-0.96	-0.78
	TO-Gr	1588.14	1588.09	1585.28	1585.32	-0.05	-2.87	-2.82
	LO-Gr	1621.28	1621.18	1616.64	1616.75	-0.1	-4.63	-4.53
GR-CNT(6,6)								
	RBM	285.01	288.28	288.06	285.10	3.27	3.04	0.08
	LO-CNT	1573.7	1573.65	1573.57	1573.65	-0.05	-0.14	-0.06
	TO-CNT	1597.27	1597.16	1596.83	1596.96	-0.11	-0.44	-0.31
	TO-Gr	1588.51	1588.45	1584.71	1584.77	-0.06	-3.8	-3.74
	LO-Gr	1621.51	1621.42	1615.42	1615.53	-0.09	-6.09	-5.97
GR-CNT(7,7)								
	RBM	244.53	248.24	247.93	244.68	3.7	3.39	0.14
	LO-CNT	1578.56	1578.5	1578.41	1578.5	-0.06	-0.15	-0.06
	TO-CNT	1603.26	1603.16	1602.46	1602.67	-0.1	-0.8	-0.59
	TO-Gr	1588.9	1588.85	1584.28	1584.31	-0.05	-4.62	-4.59
	LO-Gr	1621.57	1621.5	1614.15	1614.3	-0.07	-7.42	-7.27
GR-CNT(8,8)								
	RBM	214.08	215.79	217.66	214.11	1.71	3.58	0.03
	LO-CNT	1581.48	1581.42	1581.35	1581.39	-0.06	-0.13	-0.09
	TO-CNT	1607.48	1607.41	1606.68	1606.84	-0.08	-0.8	-0.64
	TO-Gr	1589.11	1589.06	1583.44	1583.44	-0.04	-5.67	-5.67
	LO-Gr	1621.7	1621.76	1612.79	1612.71	0.05	-8.91	-8.99
GR-CNT(9,9)								
	RBM	190.36	195.05	195.89	191.24	4.69	5.52	0.88
	LO-CNT	1583.35	1583.3	1583.3	1583.23	-0.05	-0.05	-0.12
	TO-CNT	1610.55	1610.46	1609.4	1609.68	-0.08	-1.15	-0.87
	TO-Gr	1589.3	1589.27	1582.53	1582.57	-0.03	-6.77	-6.73
	LO-Gr	1621.78	1621.7	1610.8	1611.02	-0.08	-10.98	-10.76
GR-CNT(10,10)								
	RBM	171.37	179.05	176.83	172.39	7.67	5.45	1.02
	LO-CNT	1584.64	1584.58	1584.52	1584.46	-0.06	-0.12	-0.18
	TO-CNT	1612.81	1612.73	1611.51	1611.61	-0.08	-1.3	-1.2
	TO-Gr	1589.43	1589.39	1581.77	1581.62	-0.03	-7.65	-7.81
	LO-Gr	1621.86	1621.77	1609.31	1609.31	-0.09	-12.55	-12.55
GR-CNT(11,11)								
	RBM	155.82	155.80	161.91	157.12	-0.02	6.09	1.3
	LO-CNT	1585.58	1585.51	1585.43	1585.36	-0.07	-0.15	-0.22
	TO-CNT	1614.5	1614.4	1612.86	1613.12	-0.1	-1.64	-1.38
	TO-Gr	1589.52	1589.49	1580.71	1580.72	-0.03	-8.81	-8.80
	LO-Gr	1621.92	1621.85	1607.41	1607.7	-0.07	-14.51	-14.22

Hybrids	Modes	Phonon frquencies (cm^{-1})				Total Frequency shift (cm^{-1})		
GR-CNT(8,0)		Pristine (P)	Unrelaxed hybrids(U)	Relaxed hybrids(R)	Deformed components(D)	U-P	R-P	D-P
	RBM	362.32	364.07	364.86	362.33	1.75	2.54	0
	LO-CNT	1595.1	1594.42	1594.14	1594.98	-0.68	-0.96	-0.12
	TO-CNT	1499.27	1499.15	1498.69	1498.75	-0.12	-0.58	-0.52
	TO-Gr	1502.81	1503.05	1497.78	1497.59	0.24	-5.03	-5.21
	LO-Gr	1632.25	1631.93	1629.41	1629.79	-0.33	-2.85	-2.47
GR-CNT(10,0)								
	RBM	293.14	295.86	295.87	293.2	2.72	2.72	0.06
	LO-CNT	1611.37	1610.29	1610.01	1611.26	-1.08	-1.36	-0.11
	TO-CNT	1501.05	1502.1	1501.91	1500.78	1.05	0.87	-0.27
	TO-Gr	1502.7	1503.21	1496.01	1495.51	0.52	-6.68	-7.18
	LO-Gr	1630.56	1629.91	1626.41	1627.14	-0.65	-4.15	-3.42
GR-CNT(13,0)								
	RBM	226.92	229.71	230.17	226.92	2.79	3.24	-0.01
	LO-CNT	1618.81	1617.52	1617.21	1618.67	-1.3	-1.6	-0.15
	TO-CNT	1499.4	1500.9	1500.89	1499.12	1.5	1.49	-0.28
	TO-Gr	1502.7	1503.5	1492.9	1492.08	0.81	-9.80	-10.61
	LO-Gr	1630.54	1629.63	1624.51	1625.56	-0.91	-6.03	-4.98
GR-CNT(16,0)								
	RBM	184.96	188.78	191.12	185.75	3.81	6.16	0.79
	LO-CNT	1622.71	1621.94	1620.1	1622.48	-0.77	-2.61	-0.23
	TO-CNT	1493.33	1494.42	1495.71	1492.92	1.09	2.38	-0.41
	TO-Gr	1502.7	1503.31	1489.35	1488.15	0.62	-13.35	-14.55
	LO-Gr	1630.59	1629.85	1622.83	1623.77	-0.74	-7.76	-6.82

Table 2 The phonon frequencies of pristine components, unrelaxed and relaxed hybrid nanostructures and deformed components for various SWNT-SLG systems:

S.4 Variation in phonon frequencies of pristine SWNT and SLG with charge

The variation in vibrational frequencies of individual SWNT and SLG are studied separately by introducing charges of both kinds (electrons and holes) and the results obtained are plotted in figure 1. Figure 1(a) and 1(c) show the variation in RBM, LO and TO mode frequencies of CNT(8,8) and CNT(16,0) with varying charges. The variation (asymmetric upshift with respect to electrons and holes) in RBM with introduced charges are insignificant in comparison to the LO and TO modes. In both semiconducting and metallic SWNTs, the G^- mode is affected more with the introduced charges than the G^+ mode[7–9]. It should be noted that the G^- vibrations corresponds to the LO mode vibrations in metallic tubes and TO mode vibrations in semiconducting tubes[10]. In armchair tubes and armchair-graphene chain, the vibrational frequencies of the LO and TO modes both blue-shift for the introduction of charges (both positive and negative) with the G^- mode frequencies having higher shift rates (table 3), as previously reported in literature[7,8,11–13]. The shift in TO mode (G^+) of armchair-tubes is very small in comparison to the LO mode (G^-) and asymmetric for the introduction of electrons and holes. For the frequency shift rates in zigzag-tubes and zigzag graphene chain, the G^- mode (TO mode) shows a higher shift rate with charge introduction, but the G^+ mode (LO mode) shows insignificant down-shift in comparison to the G^- mode (as shown in table 3).

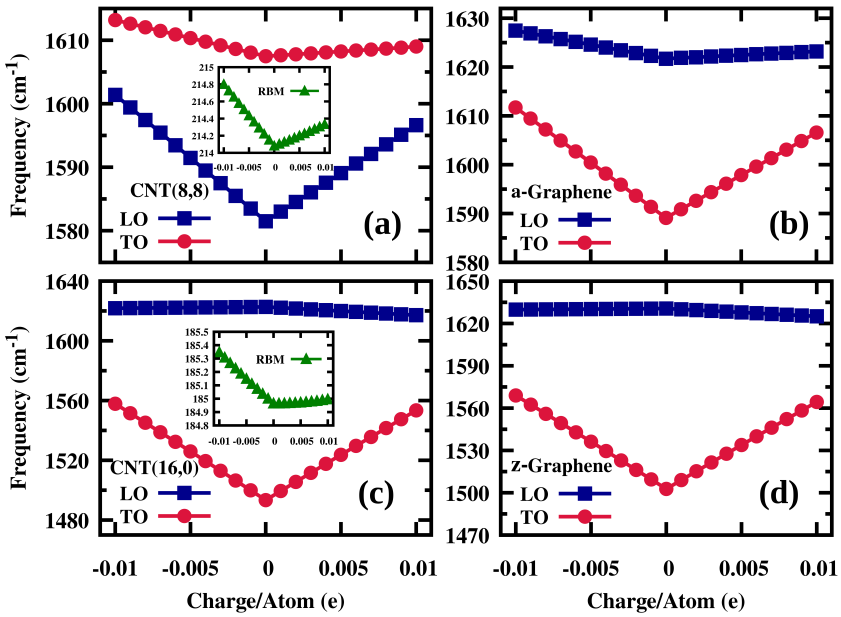

Fig. 1 Change in Raman active vibrational frequencies with varying charge in (a) CNT(8,8); (b) armchair graphene chain (with 40 atoms); (c) CNT(16,0); (d) zigzag-graphene chain (with 64 atoms). Negative charges indicate excess of electrons and positive charges indiacte excess of holes.

Hybrid System	In pristine components			In hybrid system	
	Phonon modes	Charge/atom required per cm^{-1} change (e)	Total charge required per cm^{-1} change (e)	Total charge transferred at vdW separation (e)	
GR-CNT(8,8)				Relaxed hybrid	Unrelaxed hybrid
CNT88	RBM	-0.0139	-0.4451	-0.0031	-0.0018
	TO	-0.0018	-0.0561		
	LO	-0.0005	-0.0161		
Graphene	TO	0.0006	0.0229	0.0031	0.0018
	LO	0.0067	0.2665		
GR-CNT(16,0)					
CNT160	RBM	-0.0261	-1.6710	-0.0065	-0.0034
	TO	-0.0002	-0.0099		
	LO	0.0112	0.7191		
Graphene	TO	0.0002	0.0104	0.0065	0.0034
	LO	-0.0018	-0.1162		

Table 3 Frequency shift rates with charge for pristine components of GR-CNT(8,8) and GR-CNT(16,0) hybrids and the total charge transferred at vdW separation within the hybrid systems.

References

1 M. Gaus, A. Goez and M. Elstner, *Journal of Chemical Theory and Computation*, 2013, **9**, 338–354.

2 M. Wahiduzzaman, A. F. Oliveira, P. Philipsen, L. Zhechkov, E. van Lenthe, H. A. Witek and T. Heine, *Journal of Chemical Theory and Computation*, 2013, **9**, 4006–4017.

3 T. Krüger, M. Elstner, P. Schiffels and T. Frauenheim, *The Journal of Chemical Physics*, 2005, **122**, 114110.

4 M. Elstner, *PhD dissertation*, University of Paderborn, Paderborn, Germany, 1998.

5 V. S. S. Inakollu and H. Yu, *Journal of Computational Chemistry*, 2018, **39**, 2067–2078.

6 T. A. Niehaus, S. T. A. G. Melissen, B. Aradi and S. M. V. Allaei, *Journal of Physics: Condensed Matter*, 2019, **31**, 395901.
7 A. Das, A. K. Sood, A. Govindaraj, A. M. Saitta, M. Lazzeri, F. Mauri and C. N. R. Rao, *Phys. Rev. Lett.*, 2007, **99**, 136803.
8 H. Farhat, H. Son, G. G. Samsonidze, S. Reich, M. S. Dresselhaus and J. Kong, *Phys. Rev. Lett.*, 2007, **99**, 145506.
9 A. Das and A. K. Sood, *Phys. Rev. B*, 2009, **79**, 235429.
10 M. Fouquet, H. Telg, J. Maultzsch, Y. Wu, B. Chandra, J. Hone, T. F. Heinz and C. Thomsen, *Phys. Rev. Lett.*, 2009, **102**, 075501.
11 A. Das, S. Pisana, B. Chakraborty, S. Piscanec, S. Saha, U. Waghmare, K. Novoselov, H. Krishnamurthy, A. Geim, A. Ferrari and A. Sood, *Nature nanotechnology*, 2008, **3**, 210–5.
12 K. T. Nguyen, A. Gaur and M. Shim, *Phys. Rev. Lett.*, 2007, **98**, 145504.
13 H. Farhat, K. Sasaki, M. Kalbac, M. Hofmann, R. Saito, M. S. Dresselhaus and J. Kong, *Phys. Rev. Lett.*, 2009, **102**, 126804.